

The Challenges of Incorporating Temporal and Spatial Changes into Numerical Models of Lahars

Doyle, E.E.¹, S.J. Cronin¹, S.E. Cole¹ and J.-C. Thouret²

¹ *Institute of Natural Resources, PN 432, Massey University, Private Bag 11-222, Palmerston North, N.Z.*

² *Laboratoire Magmas et Volcans, UMR 6524 CNRS, OPGC et IRD, Université Blaise Pascal, Clermont-Ferrand, France*

Email: emmadoyle79@gmail.com

Abstract: Lahars are fast moving mixtures of sediment and water. They are an extremely hazardous phenomenon in many volcanic regions, during eruptive and quiet periods. Hazard assessment and mitigation planning commonly rely upon simulations from numerical lahar models to map areas at risk. Many of these numerical models utilize a modification of existing hydrological flood, debris or granular flow equations. These commonly assume that both total volume and particulate concentration are constant, without consideration of entrainment of substrate or deposition of particles. However, lahars often go through distinct physical cycles throughout their runout, from dilute, turbulent flood waves through to laminar hyperconcentrated flows and sometimes even plug-like debris flows, often returning to waning flood waves in their final stages. Erosion, bulking and sedimentation are thought to control these phases. However, due to the scarcity of empirical data, any numerical treatment of these complex processes often involves purely theoretical functions.

We present initial results from a recent multi-parameter geophysical field study conducted in the Curah Lengkung valley, 9.5 km from the summit of Semeru Volcano, East Java. Here the channel is composed of a 30-m wide box-valley, with a base of gravel and lava bedrock. Two instrument sites were established c. 510 m apart, providing a field experiment through which active processes such as entrainment, deposition and changes in flow behaviour could be investigated. At both sites pore-pressure sensors and load cells were installed mid-channel to record the passing height and weight of the lahar, providing estimates for stage and particulate volume concentration. In addition to these mid-channel instruments, a broad-band seismograph was installed at the upstream station. This provides estimates of the sediment concentration and flow regime via seismic amplitudes, frequency responses, and signal directionality. Video footage of the lahar surface, for velocity and further stage estimates, and flow-dip samples were also collected.

A total of 8 rainfall induced lahars with durations of 1 - 3 hours were recorded. Observed flow types ranged from hyperconcentrated streamflows (<40 wt.% sediment) up to rare coarse debris flows (50-60 wt.% sediment). Flow depths were 0.5-2 m, peak velocities 3-6 m/s and maximum discharges 25-250 m³/s. The lahars are commonly characterized by a rapid onset, with surging and unsteady flow reflected in the stage records. Sediment concentration maxima lag the lahar fronts by 10-30 minutes. Typically, several large pulses or waves can be recognized and traced between the instrument sites. These provide useful markers to examine the evolution of the flow between the closely located sites, and indicate that the portions of the flow with the highest sediment concentration are accelerating in relation to the flow front. Estimates of cumulative volume for one typical event suggest that the flow is bulking during the main body of the lahar, and debulking during tail flow.

This investigation indicates that the use of two closely located geophysical instrument sites provides a critical opportunity to constrain the active physical processes within these complex flows, thus furthering both our physical understanding and their numerical description, vital for the development of hazard mitigation tools.

Keywords: *Lahar, debris flow, hyperconcentrated flow, entrainment, erosion, sedimentation, numerical modelling, geophysical instrumentation.*

1. INTRODUCTION

Sediment-rich floods and lahars are amongst the most destructive processes on volcanoes (Major & Newhall, 1989). Trigger mechanisms include crater-lake outbreaks, eruption-induced snow melting, and rainfall induced remobilization of sediment. Lahars are defined as “rapidly flowing mixtures of rock, debris and water (other than normal streamflow) from a volcano” (Smith & Fritz, 1989). They often begin as erosive watery floods that entrain sediment and water, transforming into sand-dominated hyperconcentrated flows and extremely coarse and sediment-rich debris flows. The volume and discharge of these flows increases by several times downstream during transformation. Turbulent, two-phase, hyperconcentrated flows are commonly defined by particulate volume concentrations of 20-60% (Beverage & Culbertson, 1964). They are characterised by a concentrated, boulder bearing bedload region and an upper dilute, fine-grained suspension region (Pierson & Scott, 1985; Cronin *et al.*, 1999). Debris flows are characterized by sediment concentrations above 60% and are largely unstratified, being composed of a viscoplastic mix of sediment and water, with a high yield stress (Coussot & Meunier, 1996).

Investigations of these phenomena commonly focus on artificial flume-experiments (e.g. Major, 1997) and areas where seasonal rainstorms repeatedly trigger mass flows (e.g. Arattano & Moia, 1999; Xu, 1999; Lavigne & Thouret, 2002). Due to the scarcity of empirical data, most numerical models utilise purely theoretical functions of complex processes occurring within these flows. We present initial results from a recent multi-parameter study of rainfall induced lahars conducted at Semeru Volcano, East Java, illustrating how variations in concentration influence the rheology and evolution of these flows. The use of two closely located instrument sites (c. 510 m apart) provides a critical opportunity to better characterise and understand the physical processes of such lahars.

1.1. Numerical Models

Numerical models of lahars range from those of a dilute or hyperconcentrated flow, through to those of a highly concentrated debris flow. Complex one dimensional dynamic wave theory models of sediment-rich water flows can cope with rapid changes in depth and discharge (e.g. Chen 1987; Macedonio & Pareschi 1992), assuming a constant volume and sediment concentration. Flow rheology is controlled by the energy dissipation term, being either a Manning or Chezy formula for normal stream flow. Alternatively, viscous laminar, dilatant turbulent and muddy debris flows can be modelled by relating the shear rate and the shear stress (e.g. Takahashi, 1991).

To address the important challenge of lahar bulking, Fagents and Baloga (2006) have developed a dilute model of a water-particulate continuum fluid with erosion and deposition sources. However, momentum changes are not considered. Thus, two dimensional hydrodynamic models are advantageous because they use the full mass and momentum depth-averaged shallow water equations (see summaries in Fagents & Baloga 2006 and Carrivick *et al.*, 2008). These include FLO-2D (O'Brien, 1999) and the commercially available DELFT3D model (see Carrivick *et al.*, 2008). However, simulations are limited by a lack of erosion and sedimentation in the former, and assumptions of 100% water fluid density in the latter.

To model highly concentrated debris flows, Coulomb mixture theory is often adopted. This considers a depth averaged, incompressible, constant density, pseudo-fluid (e.g. Savage & Hutter, 1989; Iverson & Denlinger, 2001). Dissipation is modelled with a Coulomb-type friction, or a coupled viscous and Coulomb type law (Wang *et al.*, 2008). Extensions include multi-dimensions (e.g. Gray *et al.*, 1999), viscous intergranular fluid (e.g. Iverson & Denlinger, 2001) and erosion and deposition (e.g. Pitman *et al.*, 2003). Recently, Pitman & Le (2005) have advanced upon the classic Savage & Hutter (1989) continuum approach, such that fluid and solid constituents are modelled independently.

2. FIELD STUDY – THE CURAH LENGKONG CHANNEL

The test site is located 9.5 km from the summit of Mt. Semeru, East Java. The Lengkong river channel is composed of a c. 30 m wide box-valley with a base of gravel and lava bedrock. This location has been used over the last 7 years (Lavigne & Thouret, 2002; Lavigne *et al.*, 2003; Lavigne & Suwa, 2004). In this investigation two sites were established c. 510 m apart: an upstream u-shaped ‘lava’ site (c. 15-20 m wide, lava bedrock base), and a downstream ‘sabo’ site (c. 25-30 m wide, concrete sabo dam). Instruments include:

- Pore pressure sensors (Hobo U20 Water Level Logger; and Solinst Levelogger Gold) installed mid-channel, recording at 10 sps at the upstream site and 2 sps downstream. When used with barometer measurements of the ambient pressure (Hobo U20 Barologger), recorded at 1 spm, the hydrostatic pressure and stage height of the lahar can be calculated.

- A 3 component Guralp CMG-6TD broadband seismometer, installed 10 m downstream of the upstream ‘lava’ site, on the true left bank. This recorded ground vibrations up to the Nyquist frequency of 62.5 Hz, and provides estimates of the sediment concentration, rheology and flow behaviour via seismic amplitudes, frequency responses, and signal directionality.
- Direct suspended load sampling was conducted at the downstream site by regularly dipping a 10 L bucket into the lahars, providing samples for estimates of particle concentration, grain size distribution and rheological properties.
- Fixed 25 fps video cameras on the true left bank of both instrument sites.

From the video camera footage, measurements of the surface flow velocity have been collected using Particle Image Velocimetry (PIV; Dalziel, 2005), in addition to qualitative measurements of the flow rheology and turbulence. Correction factors between the average body velocity and surface velocities of turbulent river flows and lahars are commonly assumed to be between 0.70 to 0.90 (e.g. Cronin *et al.*, 1999; Hayes *et al.*, 2002). A higher concentration of sediment leads to more laminar flow, as turbulent eddies are damped. For pure 1D laminar flow, 0.5 is more appropriate (Buchanan & Somers, 1969). We thus assume an average correction factor of 0.75, quoting the range of velocity and volume results for 0.65 and 0.85.

3. SPATIAL AND TEMPORAL VARIATIONS IN ACTIVE LAHARS

During the field campaign of February-March 2008, a total of 8 lahars were recorded with durations of 1 - 3 hours. The flow types ranged from hyperconcentrated streamflows up to coarse, non-cohesive, debris flows. Flow depths were 0.5 - 2 m, peak velocities 3 - 6 m/s and maximum discharges 25 - 250 m³/s. The lahars were commonly characterized by a rapid onset, with surging and unsteady flow reflected in the stage records (Fig. 1). Typically, several large pulses or waves can be recognized and traced between the instrument sites. We herein refer to these as lahar ‘packets’. Packets of this nature have previously been observed for lahars in this channel (Lavigne & Suwa, 2004) and at other locations (e.g. Arattano & Moia, 1999; Marchi *et al.*, 2002; Zanuttigh & Lamberti, 2007), and have been ascribed to upstream springs, tributary inputs, damming, ponding or surging of the flow. What ever the origin of these packets may be, they provide useful markers to examine the evolution of the flow between the closely located sites.

3.1. Stage and Particulate Concentration

Figure 2 illustrates the multi-parameter data set for the event recorded on the 5th March. Packet arrivals are observed in the wetted area (flow cross sectional area) at the upstream ‘lava’ site (Fig. 2a), in the seismic signal (Fig. 2b), and its associated energy (Fig. 2c). Bucket samples taken at the downstream ‘sabo’ site illustrate that the maximum of the sediment concentration lags the onset of the lahar by c. 33 minutes, coinciding with the head of packet 3 (Fig. 2d). Travel velocities between sites for each packet indicate that those with higher sampled sediment concentrations are propagating faster. Packet 3 has a sampled particulate concentration of c. 60% and travels at c. 4 m/s, packet 2 has a concentration of c. 48 vol.% and travels at c. 3 m/s, while packet 1 has a sampled concentration of only 26 vol.% and travels at c. 1.5 m/s. The higher concentration, faster moving packets appear to be catching up with the slower-moving flow front.

Entrainment of particles occurs downstream, increasing the flow volume (Sec. 3.3). However, we assume that the highest or lowest concentration is associated with the same packet at both sites. Thus, by utilizing the relative travel times, the timing of the downstream bucket samples is translated to the upstream lava site (Fig. 2a). The higher sediment concentrations and wetted areas of packets 2 and 3 result in the highest seismic energies (Fig. 2c). For packet 3, these high seismic energies decrease rapidly after the initial head region. However, the wetted area remains high (Fig. 2a).

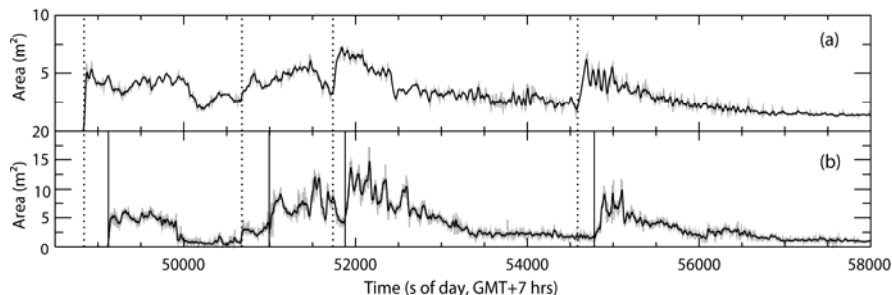


Figure 1. The wetted area (flow cross sectional area) as calculated from pore-pressure stage records at a) the upstream ‘lava’ site, and b) the downstream ‘sabo’ site on the 7th March 2008. Grey lines = full sps data, black lines = smoothed 20 s window. Dotted and solid vertical lines indicate packet arrival times at the upstream ‘lava’ and downstream ‘sabo’ sites respectively.

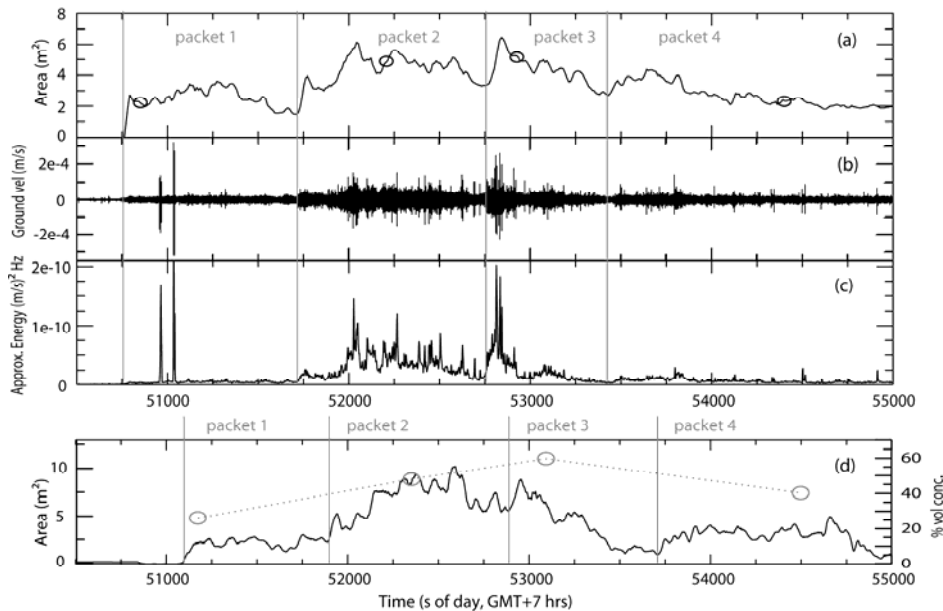


Figure 2. Upstream ‘lava’ site data on 5th March: a) 20 s smoothed wetted area, b) cross-channel component of seismic ground motion, filtered < 5Hz to remove low frequency volcanic noise, and c) spectral energy calculated from 512 point FFT velocity amplitude spectra. d) Downstream ‘sabo’ site data: 20 s smoothed wetted area (black line) and solids volume concentration inferred from bucket samples (grey circles). Open circles in (a) illustrate the equivalent sample times of the buckets at the ‘lava’ site. Travel velocities between sites are estimated at 1.5 ± 0.1 , 2.9 ± 0.2 , 4.0 ± 0.3 and 1.8 ± 0.1 m/s for each packet. Average grain size distributions of all hyperconcentrated flows indicate 0-12.9% gravel, 71.5-90% sand and 10-16% silt & clay with a Mean (Mz) size of $1.6-2.2 \phi$ ($0.33-0.22$ mm, $\phi = -\log_2(d[\text{mm}])$), Dumaisnil *et al.*, 2009).

3.2. Inferred Particle Interactions

Seismic signals generated from lahars arise from the frictional interaction of the flow with channel walls, turbulent splashing, wave-breaking and particle collisions, producing seismic signals concentrated in the 10-100 Hz range (Marcial *et al.*, 1996; Huang *et al.*, 2004; Cole *et al.*, 2009). The seismic signals produced by a sliding frictional bed load are at lower frequencies than those from particle collisions. For laboratory flows, Huang *et al.*, 2004 observed that particle collisions produced signals between 10-500 Hz, while rock-gravel bed friction was between 20-80 Hz. Cole *et al.*, 2009 identified that laminar, sliding, snow slurry lahars on Mt Ruapehu, N.Z., are dominated by frequencies of 5-20 Hz, while turbulent hyperconcentrated flows also have dominant vibrations above 30 Hz. Average spectra of each of the Semeru lahar packets are illustrated in Figure 3, for the unfiltered cross-channel seismic signal after noise removal. The highest energies are observed between 8-20 Hz, with additional peaks between 28-32 Hz, 40-45 Hz, and 55-60 Hz.

For packet 1 there is little energy in the highest frequencies (Fig. 3). This is expected for a turbulent, but dilute, flow which has few boulders available for collision. The total amplitude of the spectral signal increases with particle concentration (Figs. 2c & 3). However, even though packet 3 has a higher concentration than packet 2 (60 vs. 48 vol.%), it induces lower overall seismic energies while still having a large wetted area (Fig. 2a). This may be due to a change in rheology to quieter, denser, laminar flow. This should be characterized by less energy in the higher frequencies (Cole *et al.*, 2009). However, we observe that while packet 3 is less energetic, it still has 62% of its energy above 30 Hz. This broad frequency response suggests both frictional and collisional processes are occurring in the concentrated phases of these flows. Hence the change to higher concentrations in packet 3 was apparently not sufficient to dampen turbulence to the level observed in snow slurry lahars (Cole *et al.*, 2009). Confirmation of laminar-like flow behaviour will require future detailed analysis of the video footage and of the seismic-signal directionality.

3.3. Lahar Volumes

Figure 4 illustrates the cumulative volumes of the lahar past each site, as calculated from the PIV velocities. The greatest bulking occurs in the middle of the wave during packets 2 and the start of 3. Here the volume increases twice as fast at the downstream ‘sabo’ site than at the upstream ‘lava’ site. This may be due to entrainment of the substrate, collapse of the channel walls and the inclusion of surface rain water. While rainfall intensity is of the order of 10-20 mm/hr per m^2 , it is usually only sustained for a few tens of minutes. A direct rainfall input between sites would be in the order of 100-300 m^3 for the slowest lahars, making up a small fraction of their volume changes, which were typically $>10^3 \text{ m}^3$. During packet 4, the volume increase

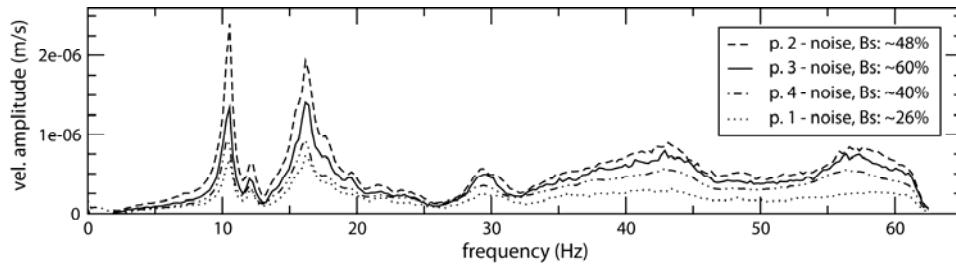


Figure 3. Average 512 point velocity amplitude seismic spectra throughout each packet, after removal of the typical noise spectrum. ‘Bs’ = sampled solids concentration at the downstream ‘sabo’ site.

at the downstream site is almost half that of the upstream site. This suggests that sedimentation and debulking of the lahar is occurring. Thus, by the end of packet 4, the total volume has changed little between sites with an increase downstream of only 10%, from 18492 ± 2466 to 20297 ± 2706 m³ (Fig. 4).

Interestingly, while the total volume of packet 2 increases 2.4 times between sites, the total volumes of packets 1, 3 and 4 decrease by 40%, 20% and 50% respectively. The decrease in the later packets (3 & 4) may be due to sedimentation in the tail of the lahar. However, it is unlikely that the initial dilute packet (1) is sedimenting. Some volume loss may occur due to water filling the pore spaces of the dry, gravel and sand substrate. In addition, the faster moving packet 2 may be consuming it (Sec 3.1). There is a shortening in the duration of packet 1 by 20% and the propagating length by 30%. If the faster moving packet (2) is just pushing and compressing it, we would expect to see a resultant rise in stage with no change in total volume. However, the volume loss we observe suggests that packet 2 is actually consuming some of packet 1.

4. DISCUSSION

Erosion and incorporation of sediment greatly influences the evolution of these flows, resulting in bulking of the flow and migration of higher concentration, faster moving portions to the flow front. Historical research into normal stream flow identifies that particle movement from the static bed occurs only when the destabilizing forces (drag, lift, buoyancy) are greater than the stabilizing force due to particle weight (see summaries in e.g. Knighton, 1988). Once in the bedload region, turbulent mixing will cause the particles to migrate into suspension. For erosion to occur, the boundary shear stress must exceed a critical value. This is often defined by the Shields parameter, which relates the shear velocity, the kinematic viscosity of water and the particle size. Laminar flow experiences a smaller shear stress than turbulent river flow, as eddy viscosity plays a lesser role (Knighton, 1988). Thus, the erosive capability is reduced. A cycle of erosion and deposition may be occurring in these rainfall induced lahars.

Preliminary video observations indicate that as the lahar progresses, surface wave breaking decreases as the flow becomes “thicker” and muddier. Remaining wave instabilities have longer wavelengths. Packet 3 is thus apparently more laminar than packets 1 and 2. The muddy texture of the flow gradually decreases throughout packet 4, with an increase in surface wave breaking, suggesting a gradual change to more turbulent flow. Due to the more turbulent nature of the dilute packet 1, basal resistance may be high. During packet 2, basal shear still exceeds the critical Shield’s parameter for erosion, resulting in considerable bulking of the flow between sites (Sec. 3.3). During packet 3 the high concentration of particles (c. 60%) may result in a gradual dampening of turbulence, leading to a seismically quieter, viscous laminar regime (Sec. 3.2). This decrease in turbulence would result in a decrease of the basal shear and thus both the erosive capability and bulking of

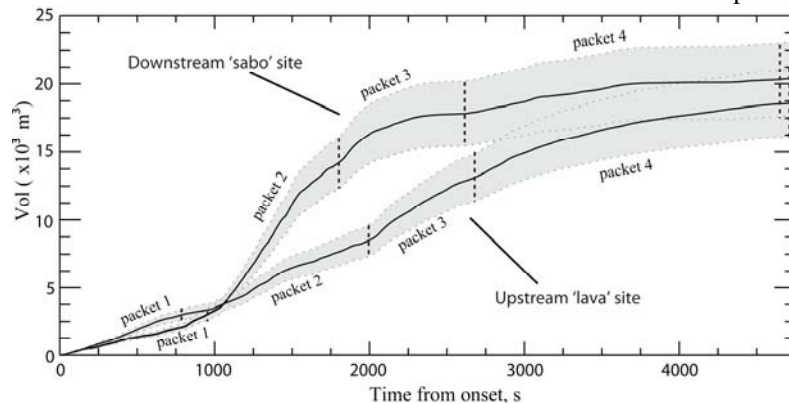


Figure 4. The cumulative volume of the rainfall induced lahar from its onset, as recorded at both sites assuming the body velocity is equal to 0.75 of the surface velocity (solid black lines). The grey regions show the range in this volume assuming a correction factor of 0.65 or 0.85 instead. Individual packets of the lahar are also annotated and distinguished by vertical dashed lines.

the flow. Sedimentation of particles is thus able to dominate at the lower boundary of the flow, such that for the slower moving packet 4, an overall debulking occurs in the lahar between sites (Sec. 3.3), accompanied by a subsequent decrease in particle concentration (Fig. 2) and a return to more turbulent flow.

Most existing lahar models consider only one dominant rheology, even if bulking is incorporated. A turbulent dilute, viscous laminar, or Coulomb-type energy dissipation term is chosen *a priori* (e.g. Macedonio & Pareschi, 1992). However, the flow behaviour changes throughout our recorded flow. During the dilute and turbulent packet (1), basal shear could be modelled as being dependent on the average velocity squared, via Manning's or Chezy's laws (Sec. 1). Turbulent and dilatant basal resistance terms that account for the shear stresses arising from particle collisions (Takahashi, 1991) would be suitable for packet 2 and packet 3. However, during the more laminar tail of packet 3 and for packet 4, basal shear may be more appropriately modelled by an empirically linear dependence upon velocity (see summary in Macedonio & Pareschi, 1992).

This interpretation considers only one event, with discrete bucket samples. Analysis of all 8 events will help confirm if this behaviour is typical. Future work will investigate the relationship between density and volume changes for periods of erosion or deposition. Analysis of the complex dependence of the seismic energy upon both the concentration of the flow and the wetted area may help identify the key seismic characteristics of laminar and turbulent flow, which may act as indicators of concentration for unsampled flows.

5. CONCLUDING REMARKS: THE OUTLOOK FOR NUMERICAL MODELS

These initial results indicate that spatial and temporal variations in rainfall induced lahars dramatically change the degree of bulking and debulking of the flow, and thus its flow behaviour. Models that incorporate bulking, concentration and volume changes are thus very promising avenues for future development (e.g. Fagents & Baloga, 2006). Recently developed models of sediment transport in river supply present an exciting opportunity for lahar modelling (e.g. Cao *et al.*, 2006). These 'coupled' models link free surface flow, sediment transport and morphological evolution, utilizing a mobile bed/flow interface to model erosion. The rate of erosion is dependent upon a threshold Shields' parameter for initiation of sediment movement. Erosion rates thus evolve with changing flow conditions. However, Manning type resistance terms and thus constant rheology are still assumed, limiting their applicability to concentrations below c. 40 vol.%.

To truly capture the rapid and complex evolution of these flows, numerical models must include volume, concentration, rheology and basal resistance changes. Only then can the full spectrum of observed behaviours be simulated. However, any model that includes this level of complexity will become extremely intensive computationally. Alternatively, development of simplified models that capture the rule-of-thumb relationships between erosion, bulking, rheology and resistance - while losing some accuracy - may usefully provide cheaper and faster hazard mitigation tools.

ACKNOWLEDGMENTS

We are grateful to Céline Dumaisnil and Yves Bru for data collection, and Emma Phillips and Kat Holt for PIV analysis. We thank the Lengkong villagers, Mahjum and Latif Usman (Bruno), for help during the field survey and Dr Gert Lube for helpful discussions. EED and SJC are supported by a Marsden Fund Research Project (MAUX0512) and a NZ Foundation for Research Science and Technology Project (MAUX0401). SEC thanks the Commonwealth Scholarship Scheme and Massey University Graduate Research School. JCT was supported by the INSU-CNRS "Hazards and global change" ACI research programme (2004-2007).

REFERENCES

- Arattano, M., and Moia, F. (1999), Monitoring the propagation of a debris flow along a torrent. *Hydrological Sciences Journal*, 44, 811-823.
- Beverage, J., and Culbertson, J. (1964), Hyperconcentrations of suspended sediment. *Journal of the Hydraulics Division, American Society of Civil Engineers*, 90, 117-126.
- Buchanan, T. J. and Somers, W. P. (1969), Discharge measurements at gauging stations. In *Techniques of water-resources investigations of the United States Geological Survey*, Book 3 in Applications of Hydraulics. U. S. Geological Survey.
- Cao, Z., Pender, G., and Carling, P. (2006), Shallow water hydrodynamic models for hyperconcentrated sediment-laden floods over erodible bed. *Advances in Water Resources*, 29, 546-557
- Carrivick, J. L., Manville, V., and Cronin, S. J. (2008), A fluid dynamics approach to modelling the 18th March 2007 lahar at Mt. Ruapehu, N.Z., *Bulletin of Volcanology*, DOI:10.1007/s00445-008-0213-2.
- Chen, C. (1987), Comprehensive review of debris flow modelling concepts in Japan. *Reviews in Engineering Geology*, 7, 13-29.

Doyle *et al.*, The challenges of incorporating temporal and spatial changes into numerical models of lahars.

- Cole, S.E., Cronin, S.J., Sherburn, S., and Manville, V. (2009), Seismic signals of snow-slurry lahars in Motion: 25 September 2007, Mt. Ruapehu, New Zealand. *Geophysical Research Letters*, doi:10.1029/2009GL038030, In press (accepted 16 April 2009).
- Coussot, P., Meunier, M. (1996). Recognition, classification and mechanical description of debris flows. *Earth Science Reviews*, 40, 209-227.
- Cronin, S.J., Neall, V.E., Lecointre, J.A. and Palmer, A.S. (1999), Dynamic interactions between lahars and stream flow: a case study from Ruapehu volcano, New Zealand., *Geological Society of American Bulletin*, 111: 28-38.
- Dalziel, S. (2005), Digiflow user guide. <http://www.damtp.cam.ac.uk/lab/digiflow/>.
- Dumaisnil, C., Thouret, J-C., Chambon, G., Doyle, E.E. and Cronin, S. J. (2009). Physical and rheological characteristics of lahar flows and deposits – A case study at Semeru volcano, Java (Indonesia). Submitted to *Earth Surface Landform and Processes*, 26 April 2009
- Fagents, S. A., and Baloga, S. M. (2006), Toward a model for the bulking and debulking of lahars, *Journal of Geophysical Research*, 111, B10201, 21 p.
- Gray, J.M.N.T., Wieland, M., and Hutter, K. (1999), Gravity driven free surface flow of granular avalanches over complex basal topography, *Proceedings of the Royal Society of London*, 455, 1841-1874.
- Hayes, S. K., Montgomery, D. R., and Newhall, C. G. (2002), Fluvial sediment transport and deposition following the 1991 eruption of Mount Pinatubo. *Geomorphology*, 45, 211–224.
- Huang, C.-J., Shieh, C.-L., and Yin, H.-Y. (2004), Laboratory study of the underground sound generated by debris flows, *Journal of Geophysical Research*, 109, F01008
- Iverson, R.M., and Denlinger, R.P. (2001), Flow of variably fluidised granular masses across three-dimensional terrain: 1. Coulomb mixture Theory. *Journal of Geophysical Research*, 106: 537-552.
- Knighton, D. (1998). *Fluvial forms and processes. A new perspective*. Arnold, London., pp 383.
- Lavigne, F., and Thouret, J-C. (2002), Sediment transport and deposition by rain-triggered lahars at Merapi volcano, Central Java, Indonesia. *Geomorphology*, 49, 45-69.
- Lavigne, F., Tirel, A., Le Froch, D., and Veyrat-Charvillon, S. (2003), A real-time assessment of lahar dynamics and sediment load based on video-camera recording at Semeru Volcano, Indonesia. In: Rickenman, D., and Chen, C.L. (eds), *Debris-Flow Hazards Mitigation: Mechanics, Prediction and Assessment*, Millpress, Rotterdam, 2, 871-882.
- Lavigne, S., and Suwa, H. (2004), Contrasts between debris flows, hyperconcentrated flows and stream flows at a channel of Mount Semeru, East Java, Indonesia. *Geomorphology*, 61, 41-58.
- Macedonio, G., and Pareschi, M.T. (1992), Numerical simulation of some lahars from Mount St. Helens. *Journal of Volcanology and Geothermal Research*, 54, 65-80.
- Major, J.J., and Newhall, C. G. (1989), Snow and ice perturbation during historical volcanic eruptions and the formation of lahars and floods; a global review. *Bulletin of Volcanology*, 52, 1-27.
- Major, J.J. (1997), Depositional processes in large-scale debris-flow experiments. *Journal of Geology*, 105, 345-366.
- Marcial, S., Melosantos, A.A., *et al.* (1996), Instrumental Lahar Monitoring at Mount Pinatubo, In: Newhall, C.G. & Punongbayan, R.S. (eds), *Fire and Mud: Eruptions and Lahars of Mount Pinatubo, Philippines*, University of Washington Press, Seattle, 1015-1022.
- Marchi, L., Arattano, M., & Deganutti, A.M. (2002), Ten years of debris-flow monitoring in the Moscardo Torrent (Italian Alps), *Geomorphology*, 46, 1-17.
- O'Brien, J.S. (1999), *FLO-2D Users Manual*. Non published reference manual, version 99.2, 157 pp.
- Pierson, T.C., and Scott, K.M. (1985), Downstream dilution of a lahar, transition from debris flow to hyperconcentrated streamflow, *Water Resources Research*, 21, 1511-1524.
- Pitman, E. B., Nichita, C.C., *et al.* (2003b), A model of granular flows over an erodible surface, *Discrete and Continuous Dynamical Systems – Series B*, 3, 589-599.
- Pitman, B.E., and Le, L. (2005), A two-fluid model for avalanche and debris flows. *Philosophical Transactions of the Royal Society, A*, 363, 1573-1601.
- Savage, S.B and Hutter, K. (1989), The motion of a finite mass of granular material down a rough incline, *Journal of Fluid Mechanics*, 199, 177-215.
- Smith, G. A. and Fritz, W. J. (1989), Volcanic influences on terrestrial sedimentation. *Geology*, 17, 375–376.
- Takahashi, T. (1991), *Debris Flow*, Balkema, A.A. (ed.), Rotterdam: IAHR Monograph Series, 165 pp.
- Wang, C., Li, S., and Esaki, T. (2008), GIS-based two dimensional numerical simulation of rainfall-induced debris flow, *Natural Hazards Earth System Science*, 8, 47-58.
- Xu, J. (1999), Erosion caused by hyperconcentrated flow on the Loess Plateau of China. *Catena*, 49, 289–307.
- Zanuttigh, B., and Lamberti, A. (2007), Instability and surge development in debris flows, *Reviews of Geophysics*, 45, RG3006.